Supporting Information:

An Improved Bioinspired Strategy to Construct Nitrogen and Phosphorus Dual-doped Network Porous Carbon with Boosted Kinetics Potassium Ion Capacitors

Chenchen Zhang [a #], Qian Li [b #], Tongde Wang [a #], Yidong Miao [a], Jiqiu Qi [a] *, Yanwei Sui [a,] *, Qingkun Meng [a], Fuxiang Wei [a], Lei Zhu [a], Wen Zhang [c], Peng Cao [c,] *

[a] *Jiangsu Province Engineering Laboratory of High Efficient Energy Storage Technology and Equipment, School of Materials and Physics, China University of Mining and Technology, Xuzhou 221116, People's Republic of China*

[b] *College of Materials Science and Engineering, Sichuan University, Chengdu, 610065, People's Republic of China*

[c] *Department of Chemical & Materials Engineering, University of Auckland, Private Bag 92019, Auckland 1142, New Zealand*

*Corresponding authors. E-mails: flower_cumt@outlook.com (Jiqiu Qi); wyds123456@outlook.com (Yanwei Sui); p.cao@auckland.ac.nz (Peng Cao)

Tel.: +86-516-83591788 Fax: +86-516-83591788

# Chenchen Zhang, Qian Li and Tongde Wang contributed equally to this manuscript.

Experimental Section

Preparation of 3D N/P co-doped meshwork carbon material

The whole synthesis process includes four parts: colloidal solution preparation, liquid nitrogen freeze-drying, high temperature carbonization and water washing. Firstly, under the condition of 80 ℃ water bath, 1g CMC-Na was slowly added into 50 ml deionized water and stirred for 2 h at the speed of 300 r/min to form aerogel like colloidal solution. Then 0.75g $(NH_4)_2HPO_4$ and 0.75g $NaNO_3$ were added into the uniform sol, and stirred for 30 min to ensure full dissolution. The sol was placed in liquid nitrogen for 1.5 min, and then the light aerogel was obtained in the vacuum freeze dryer at 72 h freeze drying (freezing condition -45℃, vacuum condition 1 Pa). Biomineralization precursors were heated at 600, 700 and 800 ℃ for 1 hour in high purity nitrogen at a flow rate of 20 $cc \cdot min^{-1}$ and a heating rate of 3 $℃ \cdot min^{-1}$. Then, the water-soluble inorganic matter on the black product is washed and filtered with deionized water. Finally, the final product NPMCs was obtained by drying the precipitate in a blast dryer at 60 ℃ for 24 hours. Through the above process, samples synthesized at different calcination temperatures (600-800 ℃) were obtained, and the samples were labeled as NPMC-600, NPMC-700 and NPMC-800. For comparison, the obtained powder was fabricated by using 1 g CMC-Na under the same preparation condition, and denoted as bare porous carbon (BPC).

Material characterizations

The morphologies and structures of the as-prepared samples were characterized by Field emission scanning electron (SEM) (SU8010) and TEM (JEOL JEM 2100F).

SEM was used to characterize the microstructure and morphology. The detailed structures of the synthesized samples were observed by Field emission transmission electron microscopy and high-resolution transmission electron microscopy (HRTEM, Tecnai F20). The crystal structure and phase composition were analyzed by X-ray diffraction (XRD) (Bruker D8) with Cu Kα radiation (λ=0.1518 nm) between 10 and 80°. Raman spectra were obtained on a RM2000 microscopic confocal Raman spectrometer (Raman, Thermo Fischer DXR). X-ray photoelectron spectroscopy (XPS, Thermo ESCALAB 250XI) was used to determine the chemical states of samples. N_2 adsorption/desorption isotherms and pore size distribution curves of carbons were obtained by Brunauere- Emmette-Teller method (BET, TriStar II 3flex).

Electrochemical performance

Potassium ion hybrid capacitors: The electrochemical performances of NPMCs were investigated using CR2032 coin cells with 0.8 M KPF_6 in EC and DEC (1:1, v/v) as electrolyte assembled in an argon glovebox. The electrodes were composed of NPMC, acetylene black and polyvinylidene fluoride with weight ratio of 8:1:1, which was coated on copper foil and dried for at least 10 h at 110 °C under vacuum. And then, to assemble the KIBs (half-cell), glass microfiber membrane (GF/D, Whatman), 0.8 M KPF_6 in EC and DEC (1:1, v/v) and potassium metal were used as the separator, electrolyte and the counter electrode, respectively. And then, the NPMC anode experienced an activation process through charge-discharge reaction for 10 cycles at the current density of 0.05 $A \cdot g^{-1}$ in a half cell. Subsequently, the pre-activated cathode was obtained from the half cell that was disassembled in the glove box. The anode was

prepared by mixing 90wt% PNAC, acetylene black and 10wt% polytetrafluoroethylene with DI water, and then the mixed materials were coated on aluminum foil, dried at 150ºC under vacuum overnight. Then, based on a preactivated NPMC cathode and PNAC anode, PICs were assembled in glove-box with 0.8 M KPF_6 in EC and DEC (1:1, v/v) as electrolyte, aluminum foil (for anode) and copper foil (for cathode) as current collectors, and glass microfiber membrane (GF/D, Whatman) as separator.

Electrochemical measurements

All working electrodes, potassium metal counter electrode and Whatman glass fibers were used to assemble 2032 model cells in an Ar-filled glove box. The electrochemical measurements of half-batteries were conducted by a LAND CT2001 test system between 0.01 and 3.0 V at room temperature. The GCD and cycling performance were tested by Land cell measurement system (Wuhan Land Electronics Co., Ltd.). Cyclic voltammetry (CV) and electrochemical impedance spectroscopy (EIS) tests were recorded in CHI 660E electrochemical workstation (Shanghai ChenHua Instrument Co., Ltd.).

Electrochemical calculations

Coin-type PIC were tested in the voltage range of 0-4.5 V. The specific capacitance, energy and power densities of PIC were calculated as described below.

Specific capacitances were calculated from GCD curves according to Eq. (1)：

$$Cm = \frac{I \times \Delta t}{m \times \Delta V} \tag{1}$$

where Cm (F g^{-1}) is the specific capacitance of a single electrode based on the mass of active material in three-electrode system or based on the total mass of active materials

in two-electrode system. I (A) is the constant charge/discharge current, Δt (s) is the discharge time, m (g) is the mass and ΔV (V) is the potential window.

Energy density (E, Wh kg^{-1}) and power density (P, W kg^{-1}) of PIC were calculated based on Eqs. (2) and (3)：

$$E = \frac{Cm \times \Delta V^2}{2 \times 3.6} \quad (2)$$

$$P = \frac{E \times 3600}{\Delta t} \quad (3)$$

Calculation Method

In this paper, all calculations were performed by means of first-principles DFT approach, using the Vienna Ab-initio Simulation Package (VASP, version 5.4.4) based on the generalized gradient approximation (GGA) with Perdew-Burke-Ernzerhof (PBE) function. [1, 2] In this calculation, the energy cut-off energy was set to 500 eV to ensure the total energy convergence; the self-consistent calculation convergence energy standard was 10^{-5} eV and the maximum mechanical convergence standard was 0.01 eV Å. To accurately estimate the metal adsorption strength and migration, dispersion correction, known as DFT-D3, was used to process van der Waals (vdW) interactions.[3] The model was built in a supercell composed of 4×4×2 carbon six-membered rings, and a 20 Å vacuum layer is set along the normal direction to prevent the interaction between atomic layers. For geometric optimization, Brillouin zone integration was performed on the Monkhorst-Pack k-point grid centered at 3×3×1Γ.

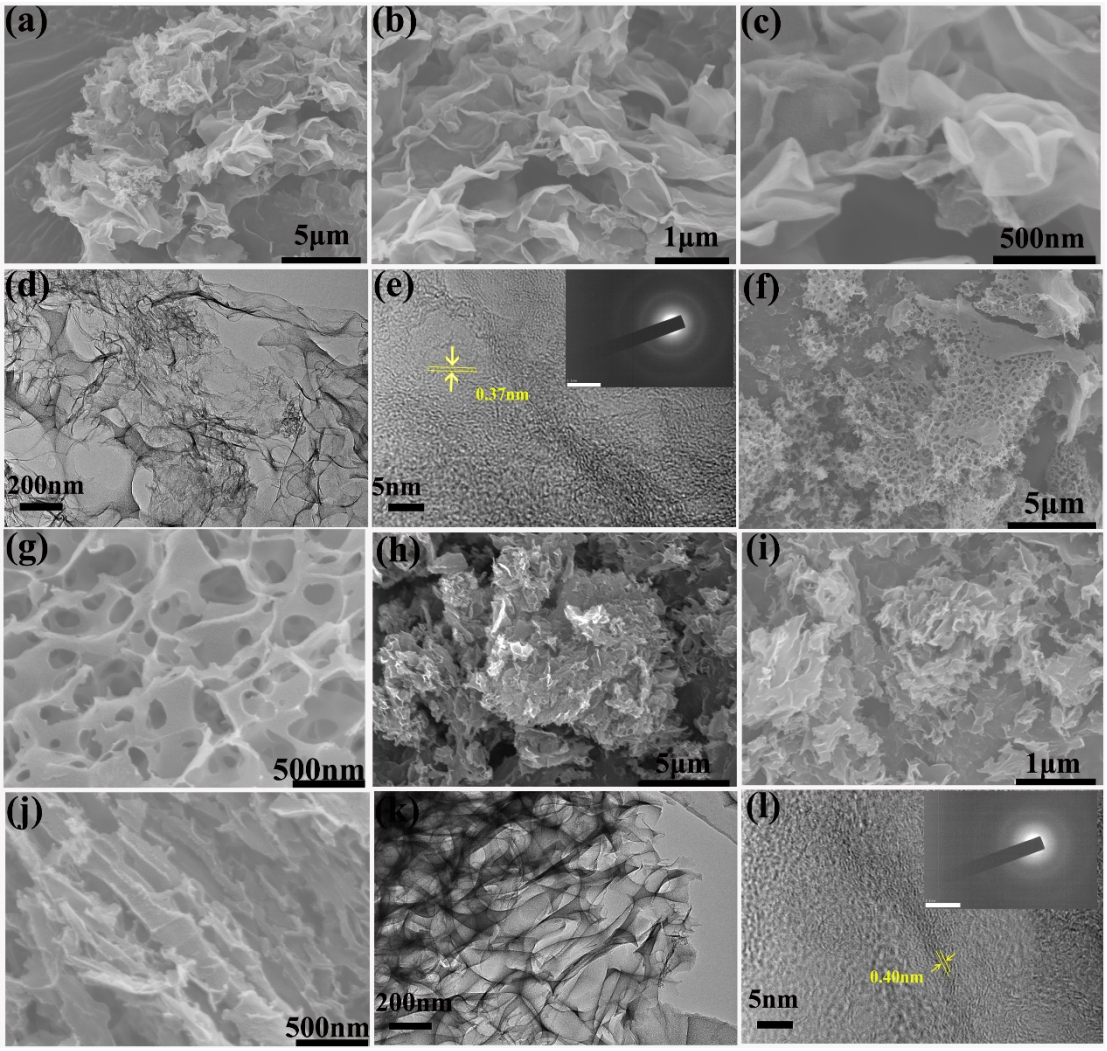

Figure S1 Morphology characterization of NPMCs; (a-c) SEM images of NPMC-600, (d) TEM images of NPMC-600 (e) high-resolution TEM image of NPMC-600, (f-g) SEM images of NPMC-700, (h-j) SEM images of NPMC-800, (k) TEM images of NPMC-800 (l) high-resolution TEM image of NPMC-800

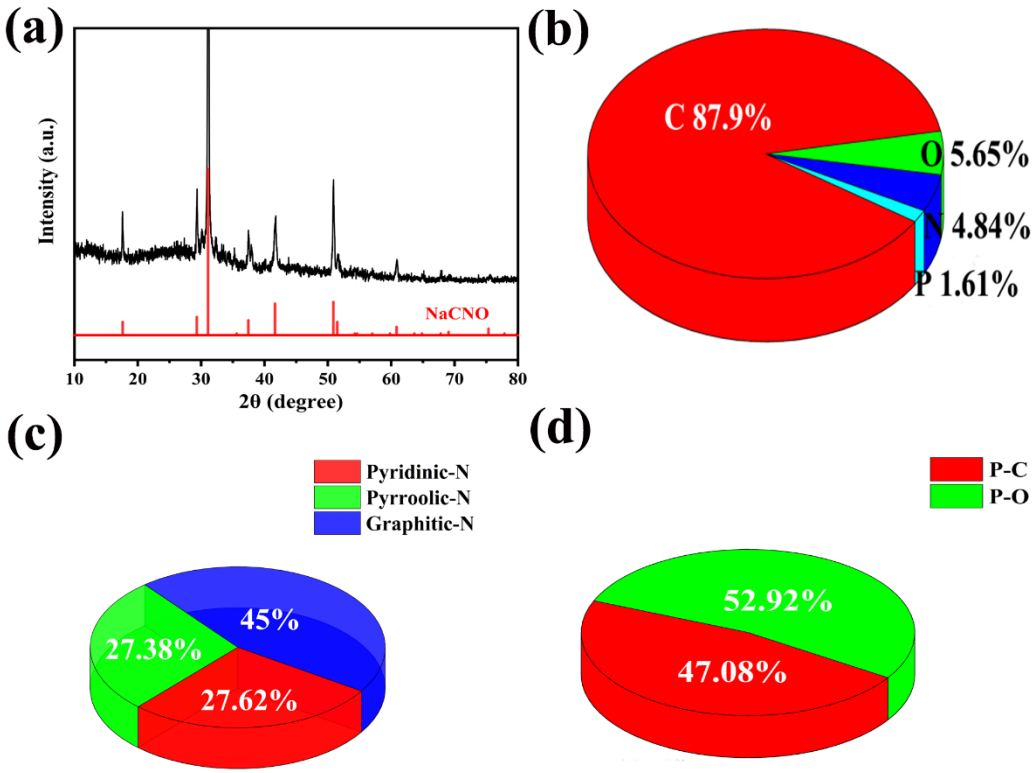

Figure S2 (a) XRD patterns of NPMCs before cleaning (b) element proportion of NPMC-700 (c) the ratio of the three N (d) the ratio of P-C to P-O

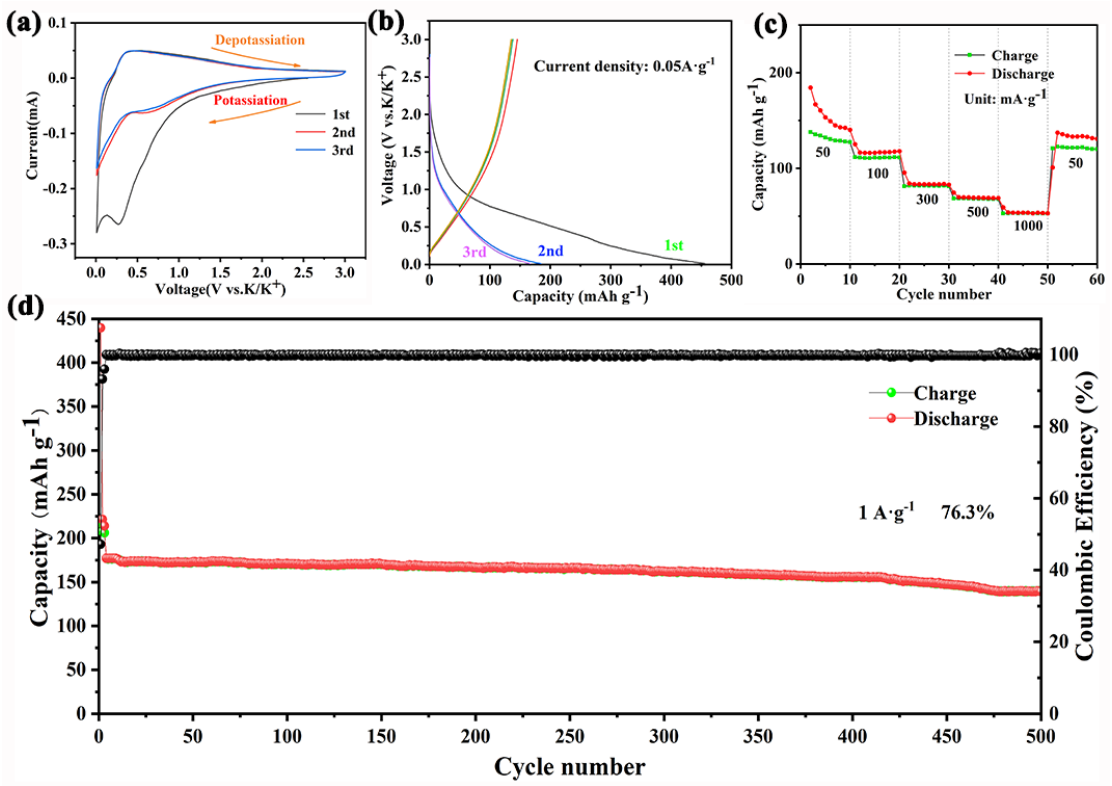

Figure S5 Electrochemical performance of BPC (a-c): (a) CV curves at 0.1 mV s^{-1} (b) Voltage profiles of initial three cycles at 0.05A g^{-1}. (c) Rate capability at various current densities; (d) cycling performance at 0.1 A·g^{-1} of NPMC-700

Table S1. Electrochemical performance comparison of the optimal NPMC anode with the previously reported carbon-based anode materials for PIBs.

Anode material	Rate capability	Cyclability
NPMC-700 (This work)	420mAh g^{-1}@0.05A g^{-1} 245 mAh g^{-1}@0.1A g^{-1} 214 mAh g^{-1}@0.3A g^{-1} 190 mAh g^{-1}@0.5A g^{-1} 173 mAh g^{-1}@1A g^{-1}	197mAh g^{-1}@0.1 A g^{-1} after 450 cycles 132 mAh g^{-1}@1 A g^{-1} after 500 cycles
wing-like porous carbon[4]	347 mAh g^{-1}@0.05A g^{-1} 301 mAh g^{-1}@0.1A g^{-1} 261 mAh g^{-1}@0.2A g^{-1} 224 mAh g^{-1}@0.5A g^{-1} 198 mAh g^{-1}@1A g^{-1}	135 mAh g^{-1}@2 A g^{-1} after 3000 cycles
Amorphous carbon[5]	278 mAh g^{-1}@0.05A g^{-1}	133 mAh g^{-1}@1 A g^{-1} after1000 cycles

	240mAh g^{-1}@0.1A g^{-1} 215 mAh g^{-1}@0.2A g^{-1} 184 mAh g^{-1}@0.5A g^{-1} 157 mAh g^{-1}@1A g^{-1}	
Nitrogen-Doped Carbon Nanosheets[6]	256.1 mAh g^{-1}@0.1A g^{-1} 203.2 mAh g^{-1}@0.2A g^{-1} 165.3 mAh g^{-1}@0.5A g^{-1} 143.8mAh g^{-1}@1A g^{-1}	236.7 mAh g^{-1}@0.1 A g^{-1} after 50 cycles
carbon mesoporous nanotubes[7]	258 mAh g^{-1}@0.1 A g^{-1} 206mAh g^{-1}@0.2A g^{-1} 169 mAh g^{-1}@0.5A g^{-1} 146mAh g^{-1}@1A g^{-1} 106mAh g^{-1}@2A g^{-1}	125 mAh g^{-1}@2 A g^{-1} after3000 cycles
Oxygen-Rich Carbon Nanosheets[8]	320 mAh g^{-1}@0.05A g^{-1} 252 mAh g^{-1}@0.1A g^{-1} 236 mAh g^{-1}@0.2A g^{-1} 213 mAh g^{-1}@0.5A g^{-1} 192 mAh g^{-1}@1A g^{-1} 173 mAh g^{-1}@2A g^{-1}	147mAh g^{-1}@2 A g^{-1} after 1300 cycles
onion-like carbon[9]	245mAh g^{-1}@0.05A g^{-1} 194 mAh g^{-1}@0.1A g^{-1} 167 mAh g^{-1}@0.2A g^{-1} 140 mAh g^{-1}@0.5A g^{-1} 121 mAh g^{-1}@1A g^{-1} 106 mAh g^{-1}@2A g^{-1} 86mAh g^{-1}@5A g^{-1} 78 mAh g^{-1}@10A g^{-1}	111 mAh g^{-1}@2 A g^{-1} after 1000 cycles
Porous Hollow Carbon[10]	280 mAh g^{-1}@0.1C 280 mAh g^{-1}@0.1C 280 mAh g^{-1}@0.1C 280 mAh g^{-1}@0.1C 280 mAh g^{-1}@0.1C 280 mAh g^{-1}@0.1C 280 mAh g^{-1}@0.1C	220 mAh g^{-1}@0.02 A g^{-1} after 200 cycles
porous carbon[11]	319 mAh g^{-1}@0.05A g^{-1} 206 mAh g^{-1}@0.1A g^{-1}	70mAh g^{-1}@1 A g^{-1} after 1000 cycles

	163 mAh g^{-1}@0.2A g^{-1} 118 mAh g^{-1}@0.5A g^{-1} 104mAh g^{-1}@0.8A g^{-1} 95 mAh g^{-1}@1A g^{-1} 78 mAh g^{-1}@2A g^{-1}	
3D N-doped framework carbon[12]	309 mAh g^{-1}@0.1A g^{-1} 247 mAh g^{-1}@0.2A g^{-1} 198mAh g^{-1}@0.5A g^{-1} 168 mAh g^{-1}@1A g^{-1} 146mAh g^{-1}@2A g^{-1} 115 mAh g^{-1}@5A g^{-1}	137mAh g^{-1}@2 A g^{-1} after 1000 cycles
Hierarchically Porous Carbon[13]	343 mAh g^{-1}@0.025A g^{-1} 273 mAh g^{-1}@0.05A g^{-1} 245mAh g^{-1}@0.1A g^{-1} 216mAh g^{-1}@1A g^{-1} 168 mAh g^{-1}@1.5A g^{-1} 152 mAh g^{-1}@2A g^{-1}	318mAh g^{-1}@0.14 A g^{-1} after 200 cycles
Dual-Carbon[14]	375 mAh g^{-1}@0.025A g^{-1} 287 mAh g^{-1}@0.05A g^{-1} 234mAh g^{-1}@0.1A g^{-1} 202 mAh g^{-1}@0.2A g^{-1} 167 mAh g^{-1}@0.5A g^{-1} 143 mAh g^{-1}@0.8A g^{-1} 115 mAh g^{-1}@1A g^{-1}	237mAh g^{-1}@0.1 A g^{-1} after 500cycles
Porous carbon nanofiber[15]	270 mAh g^{-1}@0.02A g^{-1} 190 mAh g^{-1}@2A g^{-1} 140 mAh g^{-1}@5A g^{-1} 100 mAh g^{-1}@7.7A g^{-1}	270mAh g^{-1}@0.02 A g^{-1} after 80 cycles
Highly N-doped carbon nanofibers[16]	238 mAh g^{-1}@0.1A g^{-1} 217 mAh g^{-1}@0.2A g^{-1} 192 mAh g^{-1}@0.5A g^{-1} 172 mAh g^{-1}@1A g^{-1} 153 mAh g^{-1}@2A g^{-1} 126 mAh g^{-1}@5A g^{-1}	205mAh g^{-1}@0.5 A g^{-1} after 1000 cycles 164 mAh g^{-1}@1 A g^{-1} after 2000 cycles 146 mAh g^{-1}@2 A g^{-1} after 4000 cycles
PorousHard Carbon[17]	222.8 mAh g^{-1}@0.1A g^{-1} 180.6mAh g^{-1}@0.2 A g^{-1} 140.4 mAh g^{-1}@0.5 A g^{-1}	193 mAh g^{-1}@0.1 A g^{-1} after 200 cycles

	119.7 mAh g^{-1}@0.8 A g^{-1} 94.6mAh g^{-1}@1A g^{-1} 81.6 mAh g^{-1}@2 A g^{-1}	
Coal-based carbon[18]	230 mAh g^{-1}@0.1A g^{-1} 207mAh g^{-1}@0.2 A g^{-1} 176 mAh g^{-1}@0.5 A g^{-1} 147 mAh g^{-1}@1 A g^{-1} 121mAh g^{-1}@2A g^{-1} 88 mAh g^{-1}@5 A g^{-1}	118 mAh g^{-1}@1 A g^{-1} after 1200 cycles

Table S2. Comparison on energy and power densities of this work with previously reported carbon-based electrodes for PIC.

PIC based on carbon-based electrodes	**Energy density (Wh kg^{-1})**	**Power density W kg^{-1}**	**Reference**
NPMC//AC	156.67 121.1 108.3 105.6 104.2 55.6 52.7 41.6	501 1010 1499 2080 2503 5040 9985 14965	This work
wing-like porous carbon//AC[4]	120 94 65 39 13.3	96 188 355 500 599	Adv. Mater. 2018, 30, 1800804
Amorphous Carbon //AC[5]	69.7	2041.6	Nano-Micro Lett 12
PNC-MeNT//AC[7]	175 31.6	160 3034	J. Power Sources 2017, 363, 34
PN-HPCNF //AC[19]	86	7560	Energy Environ. Sci., 2020,13, 2431-2440
3DFC//3DFC[20]	111	200	Adv. Energy

	100 85 77 67	700 1123 4798 20000	Mater., 2018, 8, 1702409.
OLC//AC[9]	142 113 106 76 55	210 800 1208 5630 21000	J. Mater. Chem. A, 7 (2019) 9247-9252
NHCS//ANHCS[21]	114.2 109.3 88 40.5 19.1	100.5 1186 2100 4658 8203	Adv. Funct. Mater., 29 (2019)
SHPNC//AC[14]	165	140	Energ. Environ. Sci., 13 (2020) 2431-2440

References

1. G. Kresse and J. J. P. r. B. Hafner, 1993, **47**, 558.
2. G. Kresse and D. J. P. r. b. Joubert, 1999, **59**, 1758.
3. S. Grimme, J. Antony, S. Ehrlich and H. J. T. J. o. c. p. Krieg, 2010, **132**, 154104.
4. Y. P. Cui, W. Liu, X. Wang, J. J. Li, Y. Zhang, Y. X. Du, S. Liu, H. L. Wang, W. T. Feng and M. Chen, *Acs Nano*, 2019, **13**, 11582-11592.
5. R. Guo, X. Liu, B. Wen, F. Liu and L. J. N.-M. L. Mai, 2020, **12**, 148.
6. W. Zong, N. B. Chui, Z. H. Tian, Y. Y. Li, C. Yang, D. W. Rao, W. Wang, J. J. Huang, J. T. Wang, F. L. Lai and T. X. Liu, *Adv Sci*, 2021, **8**.
7. J. Li, L. Yu, Y. P. Li, G. R. Wang, L. P. Zhao, B. Peng, S. Y. Zeng, L. Shi and G. Q. Zhang, *Nanoscale*, 2021, **13**, 692-699.
8. J. T. Chen, B. J. Yang, H. J. Hou, H. X. Li, L. Liu, L. Zhang and X. B. Yan, *Advanced Energy Materials*, 2019, **9**, 9.
9. J. T. Chen, B. J. Yang, H. X. Li, P. J. Ma, J. W. Lang and X. B. Yan, *J. Mater. Chem. A*, 2019, **7**, 9247-9252.
10. Z. Y. Xing, Y. T. Qi, Z. L. Jian and X. L. Ji, *ACS Appl. Mater. Interfaces*, 2017, **9**, 4343-4351.
11. X. Yu, M. J. Shao, X. M. Yang, C. X. Li, T. Li, D. Y. Li, R. T. Wang and L. W. Yin, *Chinese Chem Lett*, 2020, **31**, 2215-2218.
12. B. J. Yang, J. T. Chen, L. Y. Liu, P. J. Ma, B. Liu, J. W. Lang, Y. Tang and X. B. Yan, *Energy Storage Mater*, 2019, **23**, 522-529.
13. H. Y. Luo, M. X. Chen, J. H. Cao, M. Zhang, S. Tan, L. Wang, J. Zhong, H. L.

Deng, J. Zhu and B. G. Lu, *Nano-Micro Lett*, 2020, **12**, 13.

14. J. H. Cao, H. J. Xu, J. Zhong, X. Q. Li, S. Y. Li, Y. Y. Wang, M. Zhang, H. L. Deng, Y. L. Wang, C. Y. Cui, M. Hossain, Y. L. Cheng, L. Fan, L. Wang, T. Wang, J. Zhu and B. G. Lu, *ACS Appl. Mater. Interfaces*, 2021, **13**, 8497-8506.
15. Y. Xu, C. L. Zhang, M. Zhou, Q. Fu, C. X. Zhao, M. H. Wu and Y. Lei, *Nat Commun*, 2018, **9**, 11.
16. Y. Wang, Z. Wang, Y. Chen, H. Zhang, M. Yousaf, H. Wu, M. Zou, A. Cao and R. P. S. Han, *Adv. Mater.*, 2018, **30**.
17. W. Z. Li, R. Zhang, Z. Chen, B. B. Fan, K. K. Xiao, H. Liu, P. Gao, J. F. Wu, C. J. Tu and J. L. Liu, *Small*, 2021, **17**, 10.
18. N. Xiao, X. Y. Zhang, C. Liu, Y. W. Wang, H. Q. Li and J. S. Qiu, *Carbon*, 2019, **147**, 574-581.
19. X. Hu, G. Zhong, J. Li, Y. Liu, J. Yuan, J. Chen, H. Zhan, Z. J. E. Wen and E. Science.
20. B. Yang, J. Chen, S. Lei, R. Guo, H. Li, S. Shi and X. Yan, *Advanced Energy Materials*, 2018, **8**.
21. D. P. Qiu, J. Y. Guan, M. Li, C. H. Kang, J. Y. Wei, Y. Li, Z. Y. Xie, F. Wang and R. Yang, *Adv Funct Mater*, 2019, **29**, 8.